2025 IEEE/SICE International Symposium on System Integration (SII)
January 21-24, 2025, Munich, Germany

Development of a Versatile Structure for Mounting Drone Audition-purposed Measurement Equipment*

Yuta Tsukamoto[1], Kotaro Hoshiba[1], and Nobuyuki Iwatsuki[1]

Abstract— **Drone audition which is an audio-based searching technology is expected to be utilized for search and rescue operations in disaster areas. In this technology, the measurement equipment is required to be mounted on drones. The previous structure for mounting this equipment was designed for each drone and is costly to implement. In this paper, we propose a structure that can be universally installed on drones with a general shape. The structure was actually fabricated and confirmed its versatility by installing it on drones. Additionally the weight of the structure and measurement equipment was measured and verified its applicability by comparing the payload of a drone. We performed static load analysis and eigenvalue analysis of the structure using mechanical properties of 3D printed parts measured by three-point bending test. As a result, it was confirmed that the proposed structure has enough strength and suitable vibration characteristics to replace the previous structure.**

I. INTRODUCTION

Drones, which can move quickly regardless of ground conditions, are expected to be used for search and rescue operations in disaster areas. Many vision-based search methods using drone-embedded cameras have been studied[1], [2]. However, these methods are difficult to search for victims under poor lightning conditions or when victims are buried in rubble. To solve this problem, search methods using auditory information have been researched[3], [4], [5], [6], [7], [8], [9]. Such an audio-based technique, which localizes human-related sound sources using auditory signals recorded by a drone-embedded microphone array, is called "Drone Audition". In drone audition, it is necessary to mount the measurement equipment for sound source localization, such as sensors including microphone array, small computer and communication modules, so as not to exceed the limited payload of the drone. In addition, the microphone array needs to be designed with consideration for noises of drone's rotors and wind, and placed far from them[5], [7]. Previously, many studies have been conducted to utilize measurement equipments mounted on drones[10], [11]. However, there are few studies using measurement equipments placed far from the drone's body, as is required for drone audition.

In previous studies on drone audition, the dedicated structure for mounting these equipments on the specific drone was designed and installed directly on the drone's body[5], [6], [7], [9]. Therefore, it requires the design of a structure with the shape and dimensions corresponding to each drone, which is costly to implement.

[1]All authos are with the Department of Mechanical Engineering, Institute of Science Tokyo, 2-12-1 Ookayama, Meguro-ku, Tokyo 152-8550, Japan, {tsukamoto.y.ak, hoshiba.k.aa, iwatsuki.n.aa}@m.titech.ac.jp

In this paper, we propose a structure for mounting measurement equipment that can be universally installed on medium or large-sized drones with a landing gear. Since many of medium or large-sized industrial drones have an inverted T-shaped landing gear[12], [13] or O-shaped landing gear[14], we designed a structure that can be installed on the landing gear of the drone instead of the main body, and can also be installed on drones of different sizes and models with only simple adjustments. This structure was designed based on the following criteria: mass limitation due to the limited payload of a drone, load limitation by the weight of the equipment to be mounted, vibration characteristics against drone's vibrations during flight, and ease of adjustment for mounting equipment. This structure achieves weight reduction by combining CFRP (Carbon Fiber Reinforced Plastics) pipes and 3D printed parts, then the characteristics of the structure are dominated by these materials. Therefore, we focused on 3D printed parts, and measured the flexural modulus of two materials for FFF (Fused Filament Fabrication) and SLA (Stereo Lithography Apparatus) 3D printing by three-point bending test. Using these properties, static load analysis and eigenvalue analysis of the designed structure were performed, assuming that a microphone array and a processing unit containing small computer and other devices were mounted, to evaluate the validity of the design. In addition, the structure was actually fabricated, and its versatility was verified by installing it on two types of drones.

II. PROPOSED STRUCTURE

Many industrial drones have inverted T-shaped landing gears as shown in Fig. 1(a). By designing a structure to install on the landing gear, it can be adapted to drones with a similar shape. Therefore, we designed a structure with the shape as shown in Fig. 1(b). The landing gear and long pipe are connected in a truss shape by using short pipes and parts. A microphone array and a processing unit containing a small computer, sensors and communication modules are installed at both ends of the long pipe. The components of the structure are shown in Fig. 1(c). By adjusting the mounting angle of the central component and replacing short pipes, the structure can be installed on various drones with the shape shown in Fig1(a).

A. Design Specification for the Structure

The design specification for the structure consists of four requirements: mass limitation, load limitation, vibration characteristics, and ease of adjustment.

979-8-3315-3161-4/25/$31.00 ©2025 IEEE

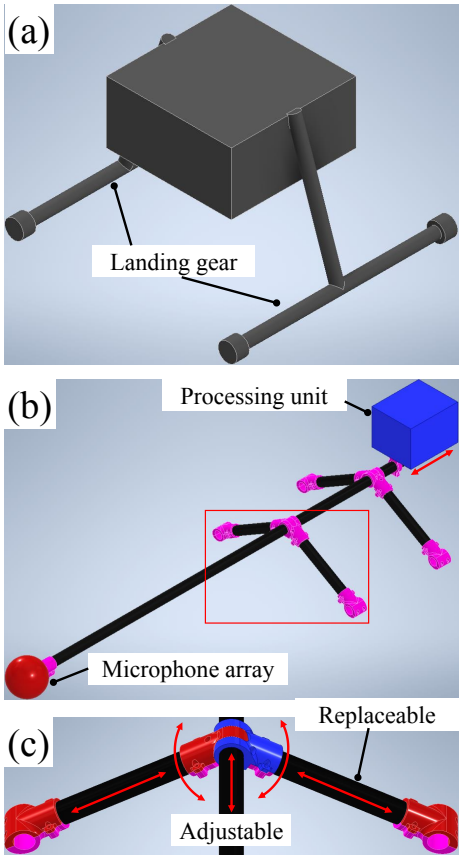

Fig. 1. (a) Standard shape of an industrial drone, (b) proposed structure for installing a microphone array and a processing unit on a drone, (c) detailed view of the area marked in red in (b).

1) Mass limitation
Due to the limited payload of drones, the structure needs to be lightweight for mounting equipment. Therefore, the structure was designed to reduce the number of components.
2) Load limitation
The structure must be strong enough to support the load generated by the weight of the equipment. Therefore, the structure was designed so that the stress caused by the weight of the equipment was less than the strength of the material.
3) Vibration characteristics
During drone flight, vibrations caused by the rotor (40 - 70 Hz and 165 - 182 Hz) and disturbances (0 - 10 Hz) are generated in the drone[15]. The structure must be designed to have appropriate tolerance for vibrations that may cause fatigue failure or component interference due to resonance. Therefore, the structure was designed to avoid a natural frequency of below 10 Hz, 40 - 70 Hz and 165 - 182 Hz.
4) Ease of adjustment
The mounting position of the microphone array needs to be adjusted to reduce the effect of drone's ego-noise. In addition, the mounting position of the processing unit also needs to be adjusted to compensate for the unbalanced center of gravity caused by the weight of the microphone array and processing unit. Therefore, the structure was designed so that the mounting position of the equipment can be easily adjusted.

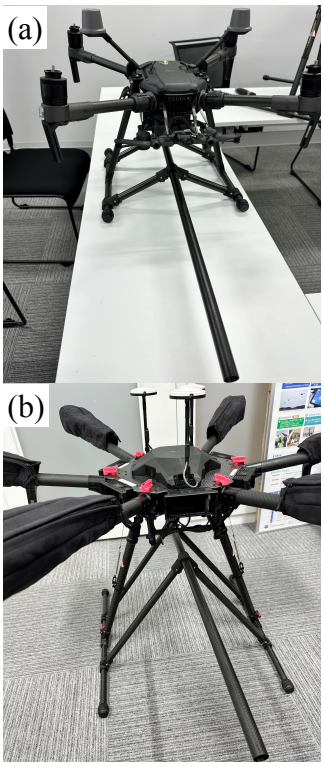

Fig. 2. Proposed structure installed on (a) DJI Matrice 210 RTK V2, (b) DJI Matrice 600 Pro.

B. Fabrication Conditions for Structure

The proposed structure has a complex shape to achieve applicability to various drones. Then, CFRP pipes were used as the main structural parts, and the parts that connecting these pipes were fabricated using a 3D printer (Onyx One, Markforged) with a filament of short carbon fiber reinforced nylon plastics (Onyx, Markforged).

The fabricated structure was installed on two drones, DJI Matrice 210 RTK V2[12] and DJI Matrice 600 Pro[13], as shown in Fig. 2. In this structure, each CFRP pipe is clamped between 3D printed parts and fixed using screws. The mounting angle of the short CFRP pipe connected to the landing gear is adjustable and short pipes are replaceable. Therefore, the structure can be installed on any drones with a landing gear by adjusting the mounting angle and the length of short pipes. The mounting position of the long CFRP pipe in the center and the processing unit is also axially adjustable, so that the positional relationship between the microphone array, the processing unit and the drone can be adjusted. The versatility of the proposed structure was confirmed by the fact that it could be installed on drones with different sizes. In addition, the mass of the fabricated structure and equipment, and the payload of the DJI Matrice 210 RTK V2 are shown in Table. I. Even though the payload of the DJI

TABLE I

MASS OF THE STRUCTURE AND EQUIPMENT AND AN EXAMPLE OF PAYLOAD OF DRONE.

	Mass [kg]
(a) Proposed structure	0.32
(b) Microphone array	0.19
(c) Processing unit	0.57
(a)+(b)+(c)	1.08
(d) Payload of drone	1.23

TABLE II

MECHANICAL PROPERTIES OF CFRP PIPE.

	CFRP pipe
Density [kg/m^3]	1550
Young's modulus [GPa]	113.6
Tensile strength [MPa]	1860
Poisson's ratio	0.3

Matrice 210 RTK V2 is lighter than that of the DJI Matrice 600 Pro, it has sufficient margin and it is confirmed that the mass of the structure is appropriate.

III. MECHANICAL PROPERTIES FOR NUMERICAL ANALYSIS

To evaluate the stress and vibration characteristics of the proposed structure, numerical analyses were performed. In the numerical analysis, it is necessary to define the mechanical properties of CFRP pipes and 3D printed parts. The CFRP pipes were assumed to be isotropic, and the nominal values[18] shown in Table. II were used as the mechanical properties. As for materials of 3D printed parts, grass fiber reinforced resin (Rigid 10K, formlabs) for the SLA 3D printing was considered in addition to Onyx. The Young's moduli of these materials were measured by three-point bending test on two types of specimens. The Poisson's ratios were determined from the literature values of general plastic materials[16], and the transverse moduli were calculated by formula using two orthogonal Young's moduli and the Young's moduli in the 45 degree direction[17].

A. Three-point bending test

Three point bending test using an autograph (AGX-20kNVD, Shimadzu) as shown in Fig. 3 was performed. The dimensions of the specimen were 10 mm in width, 10 mm in thickness, and 80 mm in length. As for test conditions, the distance between supports was set to 64 mm, the tip radius of an indenter and the support was set to 5 mm, and the test speed was set to 2 mm/min.

The specimens were prepared in four different molding directions as shown in Fig. 4, orthogonal (X-axis) and parallel (Y-axis and Z-axis) to the longitudinal direction of the specimen, 45 degree direction in XY and XZ coordinates, and 45 degree direction in YZ coordinates. The specimen of Onyx were printed using Onyx One. The in-fill rate and the wall number were set to 100% and 15, respectively. On the other hand, the specimen of Rigid 10K was printed using

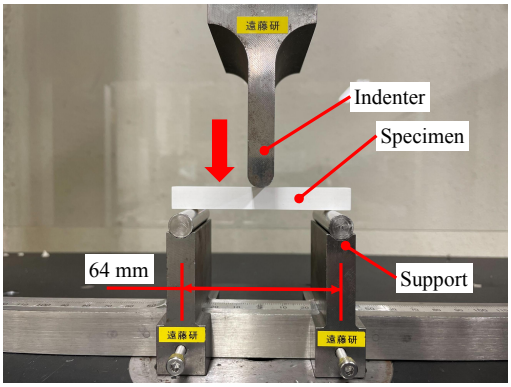

Fig. 3. Three point bending test.

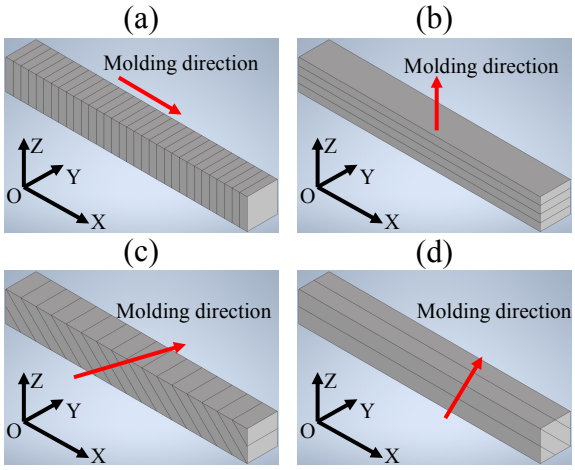

Fig. 4. Fabrication conditions of specimens. Molding direction is (a) orthogonal (X-axis), (b) parallel (Y-axis and Z-axis) to the longitudinal direction of the specimen, (c) 45 degree direction in XY and XZ coordinates, (d) 45 degree direction in YZ coordinates.

Form3. The in-fill rate was set to 100%. After printing, Rigid 10K printed parts were cleaned using a cleaning and curing machine (Mercury Plus 2.0, ELEGOO), and secondary-cured using a secondary curing machine (Form Cure, formlabs) at a curing time of 60 minutes and an internal temperature of 70 degrees of Celsius. Three specimens were evaluated for each molding condition and material.

The stress-strain curves calculated from the load and displacement obtained in the test are shown in Fig. 5. The test was terminated for Onyx when the strain reached 0.04. The bending elastic moduli, E_x, E_y and E_z, calculated using Fig. 5 are also shown in Tab. III. The bending elastic modulus of Onyx is smaller than the nominal value of 3.0 GPa[19], and is highly dependent on the molding direction. On the other hand, the bending elastic modulus of Rigid 10K is independent of the molding direction and the value is smaller than the nominal value of 9 GPa[20]. These results suggest that FFF 3D printed parts have orthotropic properties while SLA 3D printed parts have nearly isotropic properties.

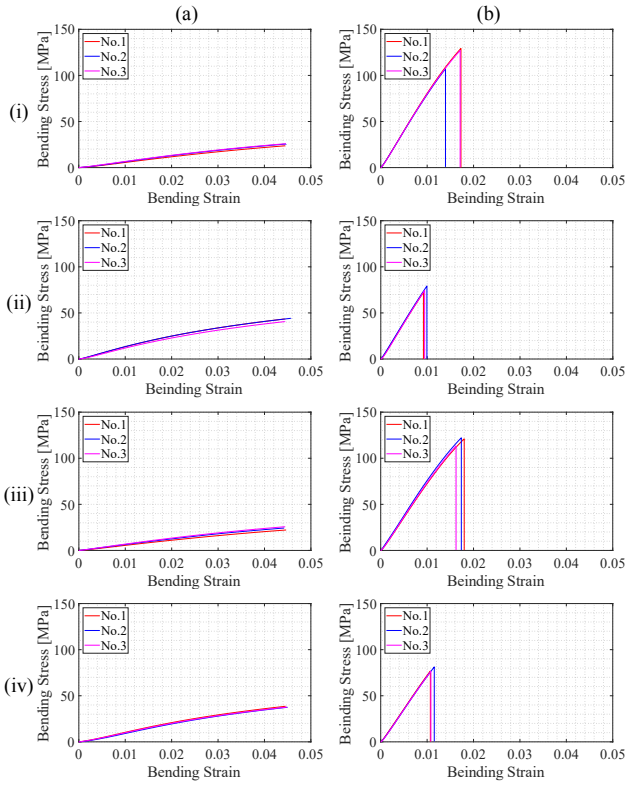

Fig. 5. Stress-strain curves. (a) Onyx, (b) Rigid 10K. Molding direction is (i) X-axis, (ii) Y-axis and Z-axis, (iii) 45 degree direction in XY and XZ coordinates, (iv) 45 degree direction in YZ coordinates.

TABLE III
MECHANICAL PROPERTIES OF 3D PRINTED PARTS USED FOR NUMERICAL ANALYSIS.

	Onyx	Rigid 10K
Density [kg/m^3]	1139	1709
Young's modulus (E_x) [GPa]	0.52	7.96
Young's modulus (E_y, E_z) [GPa]	1.20	7.99
Poisson's ratio (ν_{xy}, ν_{yz}, ν_{zx})	0.35	0.35
Transverse modulus (G_{xy}) [GPa]	0.18	2.60
Transverse modulus (G_{yz}) [GPa]	0.25	2.49
Transverse modulus (G_{zx}) [GPa]	0.21	2.60

B. Mechanical properties of each material

As for the mechanical properties of each material, Young's moduli were determined as the bending elastic moduli obtained from the three-point bending test. Poisson's ratios, ν_{xy}, ν_{yz} and ν_{zx}, were set to 0.35 based on the literature value for general plastics[16]. The transverse moduli, G_{ij}, were calculated by a formula as follows.

$$\frac{1}{G_{ij}} = \frac{4}{E_{ij,45^\circ}} - \left(\frac{1}{E_i} + \frac{1}{E_j} - \frac{2\nu_{ij}}{E_i}\right) \quad (1)$$

All mechanical properties of each material used for numerical analysis are shown in Table. III.

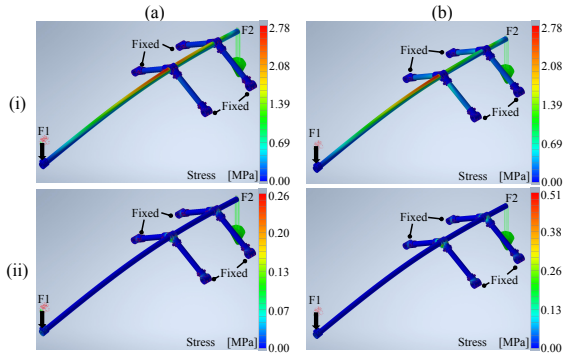

Fig. 6. Results of static load analysis. Fabricated with (a) Onyx, (b) Rigid 10K. (i) Shell elements (CFRP pipes), (ii) solid elements (3D printed parts).

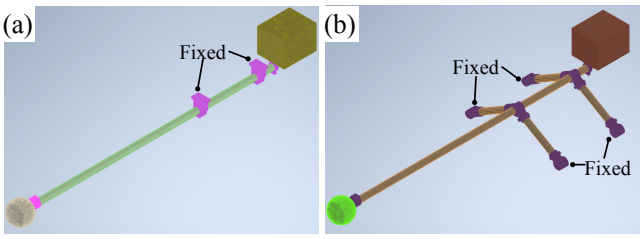

Fig. 7. Models used for eigenvalue analysis. (a) Previous structure, (b) proposed structure.

IV. NUMERICAL ANALYSIS

The stress and vibration characteristics of the proposed structure were evaluated by FEM (Finite Element Method) using Inventor Nastran, Autodesk. Mesh was generated for each part of the structure, assuming that CFRP pipes were shell elements and the 3D printed parts were solid elements. The mechanical properties of CFRP pipes and 3D printed parts obtained in Section III are used in the analysis. Under these conditions, the static load analysis considering the weight of the equipment and eigenvalue analysis for the structure only were performed. In the eigenvalue analysis, the validity of the proposed structure was verified by comparing it with the structure used in previous research.

A. Static load analysis

The following two load conditions were set, and the restraint condition was fixation at the position where the structure contact to the landing gear.

- F1 (1.3 N) generated by a microphone array mounted on the end of the long CFRP pipe.
- F2 (5.3 N) generated by a processing unit mounted on the opposite end of the long CFRP pipe.

The results of static load analysis are shown in Fig. 6. The maximum stress of shell elements was approximately 2.8 MPa while the tensile strength of CFRP pipes of 1860 MPa. The maximum stresses of solid elements were less than 0.6 MPa while the filament strengths of the 3D printed parts were over 20 MPa for Onyx and over 70 MPa for Rigid 10K as shown in Fig. 5. Therefore, it was confirmed that

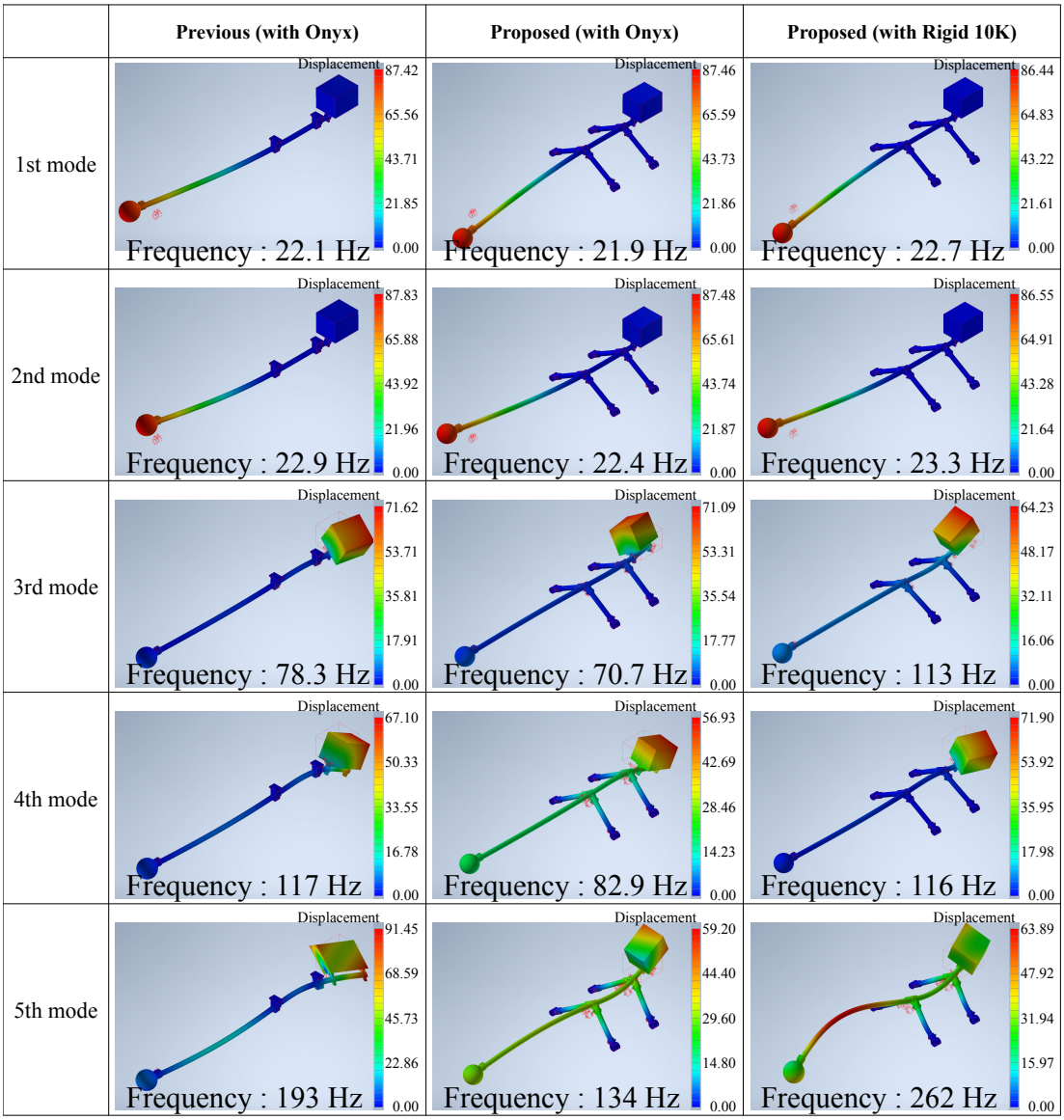

Fig. 8. Mode shapes obtained by eigenvalue analysis.

the strength of the structure was appropriate for considered loads.

B. Eigenvalue analysis

The models of previous and proposed structures including a microphone array and a processing unit used in the eigenvalue analysis are shown in Fig. 7. For the previous structure, the analysis was performed under the restraint condition that the structure is fixed at the position where the structure is attached under the main body of the drone. The analysis of the proposed structure was performed under the same restraint condition as the static load analysis.

Obtained vibration mode shapes of previous and proposed structures are shown in Fig. 8, and obtained natural frequencies are shown in Fig. 9. The analysis of the previous structure was performed using experimental properties of Onyx. The analysis result of the proposed structure using the literature properties of Onyx is added to Fig. 9 (Proposed (theoretical)).

For both structures, the first to sixth modes except for the third mode are avoided frequency bands of below 10 Hz, 40 - 70 Hz, and 165 - 182 Hz which generated in the drone. However, for the proposed structure fabricated with Onyx, the natural frequency of the third mode is close to the frequency range of 40 - 70 Hz. This could be avoided by changing the material to Rigid 10K, so it was found that fabricating with the optimum material is needed.

The difference in natural frequencies between the results of analysis using literature values and experimental values of Onyx is significant. Therefore, it is found that the effect of anisotropy is strong in 3D printing using the FFF 3D printing, even when the in-fill rate is 100%. The structure using Rigid 10K is more suitable than the structure using Onyx because its natural frequency of the fifth mode is above

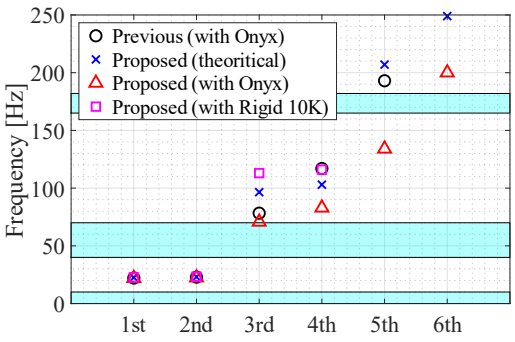

Fig. 9. Natural frequencies obtained by eigenvalue analysis. Frequency bands of vibrations that occur during drone flight are also marked in cyan.

250 Hz and all natural frequencies are avoided the frequency bands occurs in the drone. For the first and second modes, the difference in the natural frequencies due to structural and material differences is small, and the deformation of the long CFRP pipe is large, indicating that the vibration characteristics of the structure are affected by the stiffness of the long pipe. On the other hand, for the third to fifth modes, there is a difference in the natural frequencies of the previous and proposed structures. Especially for the fifth mode of the proposed structure, the entire structure is deformed, indicating that the vibration characteristics of the structure are more affected by 3D printed parts than CFRP pipes. To prevent such deformations, it was found that improvement of the stiffness of the structure by considering the shape and material is necessary.

The above results show that the structure has enough strength to withstand the loads generated by the equipment. In addition, the natural frequencies of the proposed structure, except for the third mode, avoid frequency bands of vibrations that occur during drone flight. The natural frequency of the proposed structure is similar to that of the previous structure, and the design of the proposed structure is suitable for replacing the previous structure.

V. Conclusion

In this paper, we proposed a structure for mounting measurement equipment that can be universally installed on medium or large-sized drones with a general shape to achieve the cost reduction in implementation. The structure was actually fabricated using CFRP pipes and 3D printed parts and confirmed its versatility by installing it on two types of drones. Additionally the weight of the structure and measurement equipment was measured and verified its applicability by comparing the payload of a drone. We performed static load analysis and eigenvalue analysis of the structure using mechanical properties of 3D printed parts measured by three-point bending test and nominal values. As a result, it was confirmed that the proposed structure has enough strength and suitable vibration characteristics to replace the previous structure. In this research, we focused on the structure alone during flight. However, we need to consider the assembly of a drone and the structure during flight, takeoff and landing as future works.

Acknowledgment

This work was supported by JSPS KAKENHI Grant No. JP22K14218 and F-REI No. JPFR23010102.

References

[1] A. Quan, C. Herrmann and H. Soliman, “Project Vulture: A Prototype for Using Drones in Search and Rescue Operations”, 2019 15th International Conference on Distributed Computing in Sensor Systems (DCOSS), pp. 619–624, 2019.

[2] S. Sambolek and M. Ivasic-Kos, “Automatic Person Detection in Search and Rescue Operations Using Deep CNN Detectors”, IEEE Access, vol. 9, pp. 37905–37922, 2021.

[3] K. Okutani, T. Yoshida, K. Nakamura and K. Nakadai: “Outdoor auditory scene analysis using a moving microphone array embedded in a quadrocopter”, Proc. of IEEE/RSJ International Conference on Robots and Intelligent Systems (IROS), pp. 3288–3293, 2012.

[4] T. Ohata, K. Nakamura, T. Mizumoto, T. Tezuka, K. Nakadai: “Improvement in outdoor sound source detection using a quadrotor-embedded microphone array”, Proc. of IEEE/RSJ International Conference on Robots and Intelligent Systems (IROS), pp. 1902–1907, 2014.

[5] K. Hoshiba, K. Washizaki, M. Wakabayashi, T. Ishiki, M. Kumon, Y. Bando, D. Gabriel, K. Nakadai, H. G. Okuno: “Design of UAV-Embedded Microphone Array System for Sound Source Localization in Outdoor Environments”, Sensors, vol. 17, no. 11, pp. 1–16, 2017.

[6] K. Hoshiba, K. Nakadai, M. Kumon, H. G. Okuno: “Assessment of MUSIC-Based Noise-Robust Sound Source Localization with Active Frequency Range Filtering”, J. of Robotics and Mechatronics, vol. 30, no. 3, pp. 426–435, 2018.

[7] K. Hoshiba, I. Komatsuzaki and N. Iwatsuki, “Proposal of Practical Sound Source Localization Method Using Histogram and Frequency Information of Spatial Spectrum for Drone Audition”, Drones, vol. 8, no. 4, 159, 2024.

[8] W. Manamperi, T. D. Abhayapala, J. Zhang and P. N. Samarasinghe, “Drone Audition: Sound Source Localization Using On-Board Microphones”, IEEE/ACM Transactions on Audio, Speech, and Language Processing, vol. 30, pp. 508–519, 2022.

[9] G. Yeong-Ju and J-S. Choi, “An Acoustic Source Localization Method Using a Drone-Mounted Phased Microphone Array”, Drones, vol. 5, no. 3, 75, 2021.

[10] Y. Karaca, M. Cicek, O. Tatli, A. Sahin, S. Pasli, M. F. Baser and S. Turedi, “The potential use of unmanned aircraft systems (drones) in mountain search and rescue operations”, The American Journal of Emergency Medicine, vol. 36, no. 4, pp. 583–588, 2018.

[11] M. Silvagni, A. Tonoli, E. Zenerino and M. Chiaberge, “Multipurpose UAV for search and rescue operations in mountain avalanche events”, Geomatics, Natural Hazards and Risk, vol. 8, no. 1, pp. 18–33, 2017.

[12] DJI, ”Support for Matrice 200 Series V2”, https://www.dji.com/support/product/matrice-200-series-v2

[13] DJI, ”Support for Matrice 600 Pro”, https://www.dji.com/support/product/matrice600-pro

[14] DJI, ”Phantom 4 Pro V2.0”, https://www.dji.com/en/phantom-4-pro-v2

[15] C. Ge, K. Dunno, M.A. Singh, L. Yuan and L.-X Lu, “Development of a Drone’s Vibration, Shock and Atomospheric Profiles”, Applied Sciences, vol. 11, no. 11, 5176, 2021.

[16] TORAY, ”Mechanical properties”, https://www.toplaseiko.com/oshidashi/data/

[17] N. Hazama, S. Kawabata and H. Kawai, “Analytical Method of Calculation of Orthotropic Elastic Constants of the FRP Plate”, Journal of the Society of Materials Science, Japan, vol. 16, No. 170, pp. 910–917, 1967.

[18] HOPEC, ”Technology”, https://www.hopec.jp/technology/

[19] Markforged, ”Onyx” , https://markforged.com/jp/materials/plastics/onyx

[20] formlabs, ”Formlabs Stereolithography 3D Printers Tech Specs” , https://formlabs.com/3d-printers/resin/tech-specs/